MOST FREQUENTLY USED ORSULIC LAB CELL LINES

FVB SYNGENEIC

Cell line	*Genetic alterations*	*Antibiotic resistance*	*Derivation*	*Syngeneic strain*	*Publications (see Publications sheet)*	*Suggested use*	
BR (known as BR5FVB1 Akt)	p53-/-, Brca1 -/-, myc, Akt	none	BR5FVB1 cell line was infected with RCAS-Akt	FVB IP	13, 14, 16, 18, 19, 20, 22, Fig.2	PARPi and HRD	BRCA1 -/- isogenic with C2 Kras mFVBm
BR-luc	p53-/-, Brca1 -/-, myc, Akt	puro	BR cell line was infected with Addgene - pLenti-CMVPuroLUC (w168-1)	FVB IP	6, 22, Fig.2	PARPi and HRD	BRCA1 -/- isogenic with C2 Kras mFVBm-luc

C57BL/6 SYNGENEIC

Cell line	*Genetic alterations*	*Antibiotic resistance*	*Derivation*	*Syngeneic strain*	*Publications (see Publications sheet)*	*Suggested use*	
SO-GFP-luc	p53-/-, Hras, Myc, GFP luc	neo, hygro, blast, puro	p53-/- MOSE-Hras-Myc cells were transfected with GFP-Luc	C57BL/6	Fig. 3	Oncogenes, Targeted therapies	Good for rapid tumor formation (highly aggressive) and studies of genomic instability
SO	p53-/- , Hras, Myc	neo, hygro, blast	MOSE cells from p53-/- mice were infected with Hras and myc in vitro	C57BL/6	24, Fig. 3	Oncogenes, Targeted therapies	Good for rapid tumor formation (highly aggressive) and studies of genomic instability
SO1	BRCA1 KO, p53-/-, Hras, Myc	neo, hygro, blast, puro	MOSE cells from p53-/- mice were infected with Hras and myc in vitro. BRCA1 was knocked out using Crisper Cas	C57BL/6	25	PARPi and HRD	BRCA1 knocked out (highly aggressive, high tumor mutation burden, genomic instability), isogenic to SO cells
SO1-pi1	BRCA1 KO, p53-/-, Hras, Myc	neo, hygro, blast, puro, *olaparib*	SO1 cells were grown in increasing concentration of olaparib	C57BL/6	Fig. 3, 4	PARPi and HRD	Good for understanding PARPi resistance
SO1-pi2	BRCA1 KO, p53-/-, Hras, Myc	neo, hygro, blast, puro, *olaparib*	SO1 cells were grown in increasing concentration of olaparib	C57BL/6	Fig. 3, 4	PARPi and HRD	Good for understanding PARPi resistance

ORSULIC LAB MOUSE OVARIAN CANCER CELL LINES

Cell line	Genetic alterations	Antibiotic resistance	Derivation	Syngeneic strain	Publications (see Publications sheet)	Suggested use	Existing molecular data
C1, C11, C111	p53-/-, myc, K-ras	neo	Ovaries from K5-TVA; $p53^{-/-}$ mice were infected with RCAS-myc and RCAS-K-ras in vitro; 3 independent cell lines from different mice generated at different times	N/A; grow well IP and SC in nude mice	1, 4, 8, 9, 10, 21, Fig.1	Targeted therapies	CGH, microarray
T1, T11, T111	p53-/-, myc, K-ras	neo	C1, C11, and C111 cell lines were injected IP into nude mice; T1, T11, and T111 cell lines were derived from IP tumor cells; 3 independent cell lines from different mice generated at different times	N/A; grow well IP and SC in nude mice	1, 2, 5, 8, 9, 10, 11, 21, Fig.1	Targeted therapies	CGH, microarray
C2, C22, C222	p53-/-, myc, Akt	neo	Ovaries from K5-TVA; $p53^{-/-}$ mice were infected with RCAS-myc and RCAS-Akt in vitro; ; 3 independent cell lines from different mice generated at different times	N/A; grow well IP and SC in nude mice	1, 8, 9, 10, 21, Fig.1	Targeted therapies	CGH, microarray
T2, T22, T222	p53-/-, myc, Akt	neo	C2, C22, and C222 cell lines were injected IP into nude mice; T2, T22, and T222 cell lines were derived from IP tumor cells; ; 3 independent cell lines from different mice generated at different times	N/A; grow well IP and SC in nude mice	1, 2, 5, 8, 9, 10, 11, 12, 21, Fig.1	Targeted therapies	CGH, microarray
C3	p53-/-, Akt, K-ras	neo	Ovaries from K5-TVA; $p53^{-/-}$ mice were infected with RCAS-Akt and RCAS-K-ras in vitro	N/A; grow slowly IP and SC in nude mice	3, 7, 10, Fig.1	Myc and PVT1 amplification - after IP injection into nude mice, the tumor clones will develop different types of Myc and PVT1 amplifications	CGH
T3 (Multiple clones available)	p53-/-, Akt, K-ras	neo	C3 cell line was injected IP into nude mice; T3 cell lines was derived from IP tumor cells	N/A; grow well IP and SC in nude mice	2, 3, 7, 10, 11, Fig.1	Myc and PVT1 amplification - after IP injection into nude mice, the tumor clones developed different types of Myc and PVT1 amplifications	CGH
BR2, BR5, BR6	p53-/-, Brca1 -/-, myc	none	Ovaries from K5-TVA; $p53^{F/F}$; $Brca1^{F/F}$ mice were infected with RCAS-Cre and RCAS-myc in vitro; 3 independent experiments from different mice at different times	N/A; grow well IP and SC in nude mice	10, 12; Fig.1	PARPi and HRD	CGH, microarray
TBR2, TBR5, TBR6	p53-/-, Brca1 -/-, myc	none	BR2, BR5, and BR6 cell lines were injected IP into nude mice; TBR2, TBR5, and TBR6 cell lines were derived from IP tumor cells; ; 3 independent cell lines from different mice generated at different times	N/A; grow well IP and SC in nude mice	2, 10, 11, Fig.1	PARPi and HRD	CGH, microarray
BR6 FVB1	p53-/-, Brca1 -/-, myc	none	BR6 cell line was injected IP into FVB mice; BR6 FVB1 was derived from IP tumor cells	FVB IP		PARPi and HRD	
BR5 FVB1, BR5 FVB2	p53-/-, Brca1 -/-, myc	none	BR5 cell line was injected IP into FVB mice; BR5FVB1, BR5FVB2 cell lines were derived from IP tumor cells	FVB IP	12, 15, 17	PARPi and HRD	
BR (known as BR5FVB1 Akt)	p53-/-, Brca1 -/-, myc, Akt	none	BR5FVB1 cell line was infected with RCAS-Akt	FVB IP	13, 14, 16, 18, 19, 20, 22, Fig.2	PARPi and HRD	
BR-luc	p53-/-, Brca1 -/-, myc, Akt, luc	puro	BR cell line was infected with Addgene - pLenti-CMVPuroLUC (w168-1)	FVB IP	6, 22, Fig.2	PARPi and HRD	
BR Kras	p53-/-, Brca1 -/-, myc, Akt, Kras	puro	BR cell line was infected with Addgene -pBabe-puro-K-Ras V21 (plasmid #9052)	FVB IP		PARPi and HRD	
BR Hras	p53-/-, Brca1 -/-, myc, Akt, Hras	hygro	BR cell line was infected with Addgene -pWzl-hygro-H-Ras V12 (plasmid #18749)	FVB IP		PARPi and HRD	
C2 + K-ras	p53-/-, myc, Akt, K-ras	neo	C2 cell line was infected with RCAS-K-ras	FVB IP		PARPi and HRD	
C2 Kras mFVBm	p53-/-, myc, Akt, K-ras	neo	C2 + K-ras cell line was injected into a nude mouse; IP tumor nodule was isolated, expanded and injected into an FVB mouse; IP tumor nodule was isolated from the FVB mouse	FVB IP		PARPi and HRD	
C2 Kras mFVBm-luc	p53-/-, myc, Akt, K-ras	neo, puro	C2 + K-ras cell line was injected into a nude mouse; IP tumor nodule was isolated, expanded and injected into an FVB mouse; IP tumor nodule was isolated from the FVB mouse. The resulting C2 Kras mFVBm cell line was infected with Addgene - pLenti-CMVPuroLUC (w168-1)	FVB IP		PARPi and HRD	
C2 + Her-2	p53-/-, myc, Akt, Her-2	neo	C2 cell line was infected with RCAS-Her-2	N/A; grow well IP and SC in nude mice		Oncogenes, Targeted therapies	
C2 + MT	p53-/-, myc, Akt, MT	neo	C2 cell line was infected with RCAS-middle T	N/A; grow well IP and SC in nude mice		Oncogenes, Targeted therapies	
T2 + K-ras	p53-/-, myc, Akt, K-ras	neo	T2 cell line was infected with RCAS-K-ras	N/A; grow well IP and SC in nude mice		Oncogenes, Targeted therapies	
T2 + Her-2	p53-/-, myc, Akt, Her-2	neo	T2 cell line was infected with RCAS-Her-2	N/A; grow well IP and SC in nude mice		Oncogenes, Targeted therapies	
T2 + MT	p53-/-, myc, Akt, Her-2	neo	T2 cell line was infected with RCAS-middle T	N/A; grow well IP and SC in nude mice		Oncogenes, Targeted therapies	
mT2 + K-ras	p53-/-, myc, Akt, K-ras	neo	T2 + K-ras cells were injected IP into FVB mice; mT2+K-ras was derived from IP tumor cells	N/A; grow well IP and SC in nude mice	12	Oncogenes, Targeted therapies	
T2 + K-ras-pMSCV-puro-Luc+	p53-/-, myc, Akt, K-ras	neo, puro	T2 + K-ras cells were injected IP into FVB mice; mT2+K-ras was derived from IP tumor cells. The cells were then infected with pMSCV-puro-luc+ and selected by puromycin	N/A; grow well IP and SC in nude mice	12	Oncogenes, Targeted therapies	
T22 + H-ras	p53-/-, myc, Akt, H-ras	neo, puro	T22 cell line was infected with pBabe-puro-Ha-rasV12, then selected by puromycin	N/A; grow well IP and SC in nude mice	2, 5, 12	Oncogenes, Targeted therapies	
T22 + H-ras-MIG-W-Luc+	p53-/-, myc, Akt, H-ras	neo, puro	T22 cell line was infected with pBabe-puro-Ha-rasV12, then selected by puromycin. The cells were infected with MIG-W-Luc+ and sorted by FACS	N/A; grow well IP and SC in nude mice	2, 5, 12	Oncogenes, Targeted therapies	
T22 + pBabe	p53-/-, myc, Akt	neo, puro	T22 cell line was infected with pBabe-puro, then selected by puromycin	N/A; grow well IP and SC in nude mice	5	Oncogenes, Targeted therapies	
T22 + pBabe-K-ras	p53-/-, myc, Akt, K-ras	neo, puro	T22 cell line was infected with pBabe-puro-K-rasG12D, then selected by puromycin	N/A; grow well IP and SC in nude mice	5	Oncogenes, Targeted therapies	
mC1 + GFP (4 cell lines)	p53-/-, myc, K-ras, GFP	neo	C1 cell line was injected IP into four nude mice; RCAS-GFP was injected IP; one mC1+GFP cell line was derived from IP tumor cells from each mouse	N/A; grow well IP and SC in nude mice		Oncogenes, Targeted therapies	
mC1 + Akt (4 cell lines)	p53-/-, myc, K-ras, Akt	neo	C1 cell line was injected IP into four nude mice; RCAS-Akt was injected IP; one mC1+Akt cell line was derived from IP tumor cells from each mouse	N/A; grow well IP and SC in nude mice		Oncogenes, Targeted therapies	
pBmyc	p53F/F, Brca1 -/-, myc	none	Ovaries from K5-TVA; $p53^{-/-}$; $Brca1^{-/-}$ mice were infected with RCAS-myc in vitro	N/A; grow well IP and SC in nude mice		Oncogenes, Targeted therapies	
$p53^{-/-}$ + myc + Her-2	p53-/-, myc, Her-2	neo	Ovaries from K5-TVA; $p53^{-/-}$ mice were infected with RCAS-myc and RCAS-Her-2 in vitro	N/A; grow well IP and SC in nude mice		Oncogenes, Targeted therapies	
$p53^{-/-}$ + myc + MT	p53-/-, myc, MT	neo	Ovaries from K5-TVA; $p53^{-/-}$ mice were infected with RCAS-myc and RCAS-middle T in vitro	N/A; grow well IP and SC in nude mice		Oncogenes, Targeted therapies	

$p53^{-/-}$ + myc + cyclin D1	p53-/-, myc, cyclin D1	neo	Ovaries from K5-TVA; $p53^{-/-}$ mice were infected with RCAS-myc and RCAS-cyclinD1 in vitro	N/A; grow well IP and SC in nude mice		Oncogenes, Targeted therapies
$p53^{-/-}$ tet-O-myc + Akt	p53-/-, myc, Akt	neo	Ovaries from K5-TVA; $p53^{-/-}$; tet-O-myc mice were infected with RCAS-Akt and RCAS-rtTA in vitro in the presence of doxycycline	N/A; grow well IP and SC in nude mice		Oncogenes, Targeted therapies
$p53^{-/-}$ + Akt + Her-2	p53-/-, Akt, Her-2	neo	Ovaries from K5-TVA; $p53^{-/-}$ mice were infected with RCAS-Akt and RCAS-Her-2 in vitro	N/A; grow well IP and SC in nude mice		Oncogenes, Targeted therapies
$p53^{-/-}$ + Akt + MT	p53-/-, Akt, MT	neo	Ovaries from K5-TVA; $p53^{-/-}$ mice were infected with RCAS-Akt and RCAS-MT in vitro	N/A; grow well IP and SC in nude mice		Oncogenes, Targeted therapies
T-$p53^{-/-}$ + myc + Her-2	p53-/-, myc, Her-2	neo	$p53^{-/-}$ + myc + Her-2 cell line were injected IP into nude mice; T-$p53^{-/-}$ + myc + Her-2 cell line were derived from IP tumor cells	N/A; grow well IP and SC in nude mice		Oncogenes, Targeted therapies
T-$p53^{-/-}$ + myc + MT	p53-/-, myc, MT	neo	$p53^{-/-}$ + myc + MT cell line were injected IP into nude mice; T-$p53^{-/-}$ + myc + MT cell line were derived from IP tumor cells	N/A; grow well IP and SC in nude mice		Oncogenes, Targeted therapies
T-$p53^{-/-}$ + Akt + Her-2	p53-/-, Akt, Her-2	neo	$p53^{-/-}$ + Akt + Her-2 cell line were injected IP into nude mice; T-$p53^{-/-}$ + Akt + Her-2 cell line were derived from IP tumor cells	N/A; grow well IP and SC in nude mice		Oncogenes, Targeted therapies
T-$p53^{-/-}$ + Akt + MT	p53-/-, Akt, MT	neo	$p53^{-/-}$ + Akt + MT cell line were injected IP into nude mice; T-$p53^{-/-}$ + Akt + MT cell line were derived from IP tumor cells	N/A; grow well IP and SC in nude mice		Oncogenes, Targeted therapies
p53-/-	p53-/-	neo	MOSE cells from p53-/- mice	Do not form tumors in mice		Oncogenes, Targeted therapies
p53-/- Hras	p53-/-, Hras	neo, hygro	MOSE cells from p53-/- mice were infected with Hras in vitro	2M cells form IP tumors in 21-35 days in Nu/Nu and C57BL/6 syngeneic mice	Fig. 3	Oncogenes, Targeted therapies
p53-/- Myc	p53-/-, Myc	neo, blast	MOSE cells from p53-/- mice were infected with myc in vitro	2M cells form IP tumors in108-150 days in Nu/Nu and C57BL/6 syngeneic mice	Fig. 3	Oncogenes, Targeted therapies
p53-/- Hras Myc	p53-/- , Hras, Myc	neo, hygro, blast	MOSE cells from p53-/- mice were infected with Hras and myc in vitro	2M cells form IP tumors in 14-18 days in Nu/Nu and C57BL/6 syngeneic mice	Fig. 3	Oncogenes, Targeted therapies
p53-/- Hras GFP luc	p53-/-, Hras, GFP luc	neo, hygro, puro	p53-/- MOSE-Hras cells were transfected with GFP-Luc	2M cells form IP tumors in 21-35 days in Nu/Nu and C57BL/6 syngeneic mice	Fig. 3	Oncogenes, Targeted therapies
p53-/- Ccne1	p53-/-, Ccne1	neo, puro	MOSE cells from p53-/- mice were infected with CCNE1 in vitro	2M cells form IP tumors in 158-293 days in Nu/Nu and C57BL/6 syngeneic mice	Fig. 3	Oncogenes, Targeted therapies
p53-/- Hras Ccne1	p53-/-, Hras, Ccne1	neo, hygro, puro	MOSE cells from p53-/- mice were infected with Hras and CCNE1 in vitro	2M cells form IP tumors in about 31 days in Nu/Nu and C57BL/6 syngeneic mice	Fig. 3, 4	Oncogenes, Targeted therapies
p53-/- Myc Ccne1	p53-/-, Myc, Ccne1	neo, blast, puro	MOSE cells from p53-/- mice were infected with myc and CCNE1 in vitro	2M cells form IP tumors in 62 – 70 days in Nu/Nu and C57BL/6 syngeneic mice	Fig. 3	Oncogenes, Targeted therapies
SO	p53-/- , Hras, Myc	neo, hygro, blast	MOSE cells from p53-/- mice were infected with Hras and myc in vitro	1M cells form IP tumors in C57BL/6 syngeneic mice in 2-3 weeks	24, Fig. 3	PARPi and HRD
SO1	BRCA1 KO, p53-/-, Hras, Myc	neo, hygro, blast, puro	MOSE cells from p53-/- mice were infected with Hras and myc in vitro. BRCA1 was knocked out using Crisper Cas	1M cells form IP tumors in C57BL/6 syngeneic mice in 2-3 weeks	25	PARPi and HRD
SO1-pi1	BRCA1 KO, p53-/-, Hras, Myc	neo, hygro, blast, puro, olaparib	SO1 cells were grown in increasing concentration of olaparib	not tested		PARPi and HRD
SO1-pi2	BRCA1 KO, p53-/-, Hras, Myc	neo, hygro, blast, puro, olaparib	SO1 cells were grown in increasing concentration of olaparib	not tested		PARPi and HRD

Mouse ovarian cancer cell lines with defined initiating genetic alterations

The ability to introduce multiple oncogenic alterations into ovarian cells provides very efficient means in which to evaluate the cooperation of candidate genes in ovarian oncogenesis. In order to simulate the cooperation of several biochemical pathways in cancer development, we have engineered mouse ovarian cancer cell lines with different combinations of defined alterations in genes such as p53, Brca1, c-myc, K-ras, and Akt (Fig. 1A and B). Syngeneic or nude mice injected with transformed primary cell lines develop tumors that closely resemble human ovarian tumor development and metastatic spread (Fig. 1C). Histologically, these tumors resemble human metastatic ovarian serous papillary carcinoma, which is the most common tumor type in ovarian cancer patients (Fig. 1D). Unlike human tumors that are thought to develop over several years, the mouse tumors develop within several weeks. During this time, the transformed cells likely accumulate genetic aberrations that facilitate their survival, proliferation, dissemination and attachment to intraperitoneal organs. Each tumor-bearing mouse was used to develop one ovarian cancer cell line (T and TBR cell lines, Fig. 1).

Fig. 1. Derivation of mouse ovarian cancer cell lines with defined initiating genetic alterations. A) Derivation of cancer cell lines that contain various combinations of genetic alterations in p53, c-myc, K-ras and Akt. B) Derivation of cancer cell lines that contain a combination of genetic alterations in p53, Brca1 and c-myc. C) Injection of primary transformed cell lines results in intraperitoneal carcinomatosis. Each tumor cell line was derived from a single tumor nodule. D) H&E staining of intraperitoneal tumors in mice.

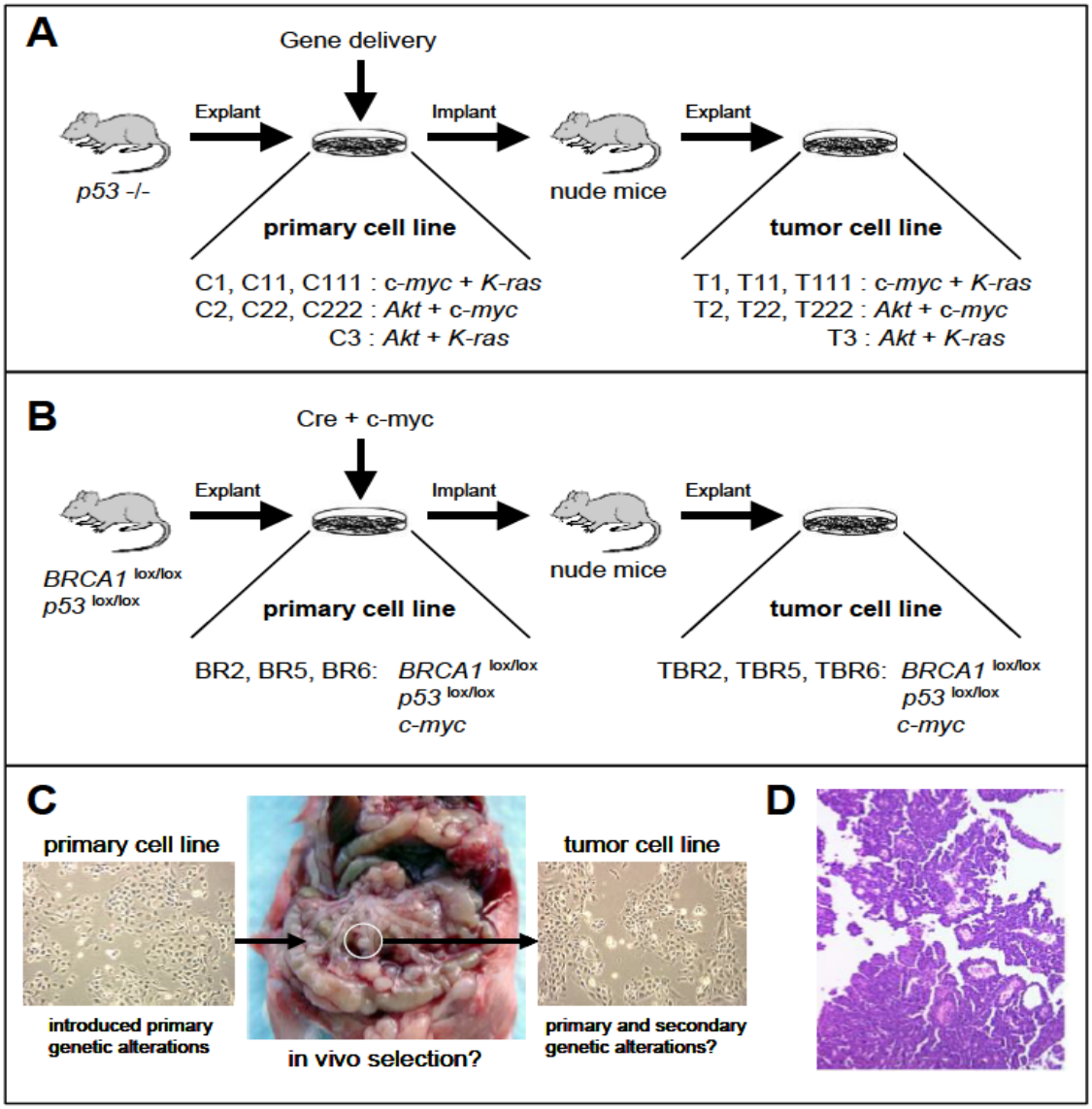

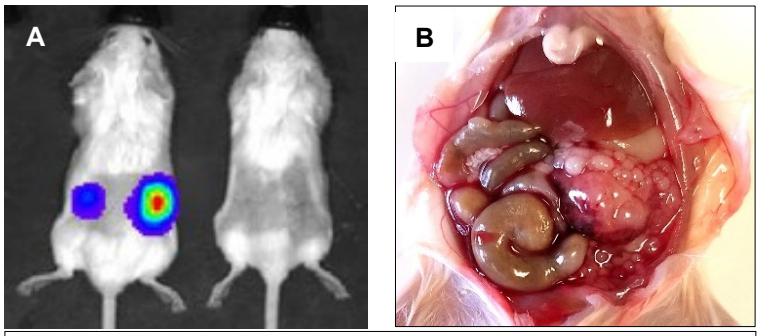

Fig. 2. An FVB syngeneic mouse ovarian cancer model. **(A)** Imaging of luciferase-tagged cells 10 days after orthotopic implantation of mouse ovarian cancer cells BR-luc (left) and BR (right). **(B)** Intraperitoneal tumor growth. Five weeks after intraperitoneal injection of $5x10^6$ BR-luc cells, mice are bloated with ascites. Most of the tumor burden is located to the omentum.

Fig. 3

GENERATION OF CELL LINES

FIGURES: Dr. Hasmik Agadjanian

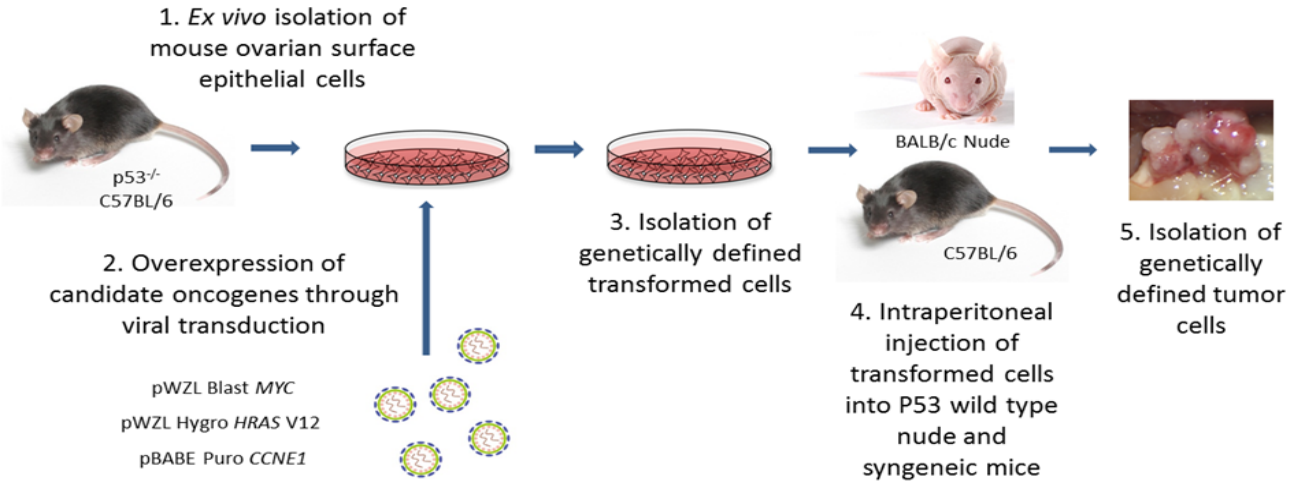

CELL MORPHOLOGY

C57BL/6 syngeneic mouse ovarian cancer cell lines with different morphologies (Hras makes cells senescent or spindle-shaped as has been shown in many epithelial cell types)

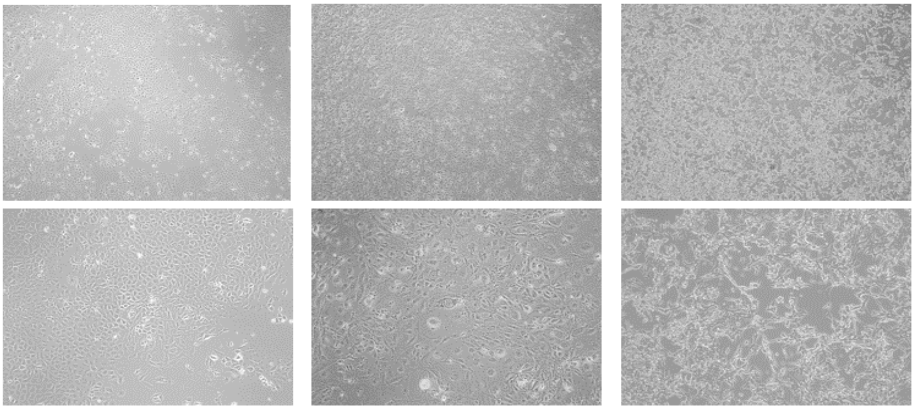

p53-/- Myc
cobblestone-shaped

p53-/- Hras
senescent and spindle-shaped

p53-/- Myc Hras
spindle-shaped and round, grow in 3D

Fig. 4

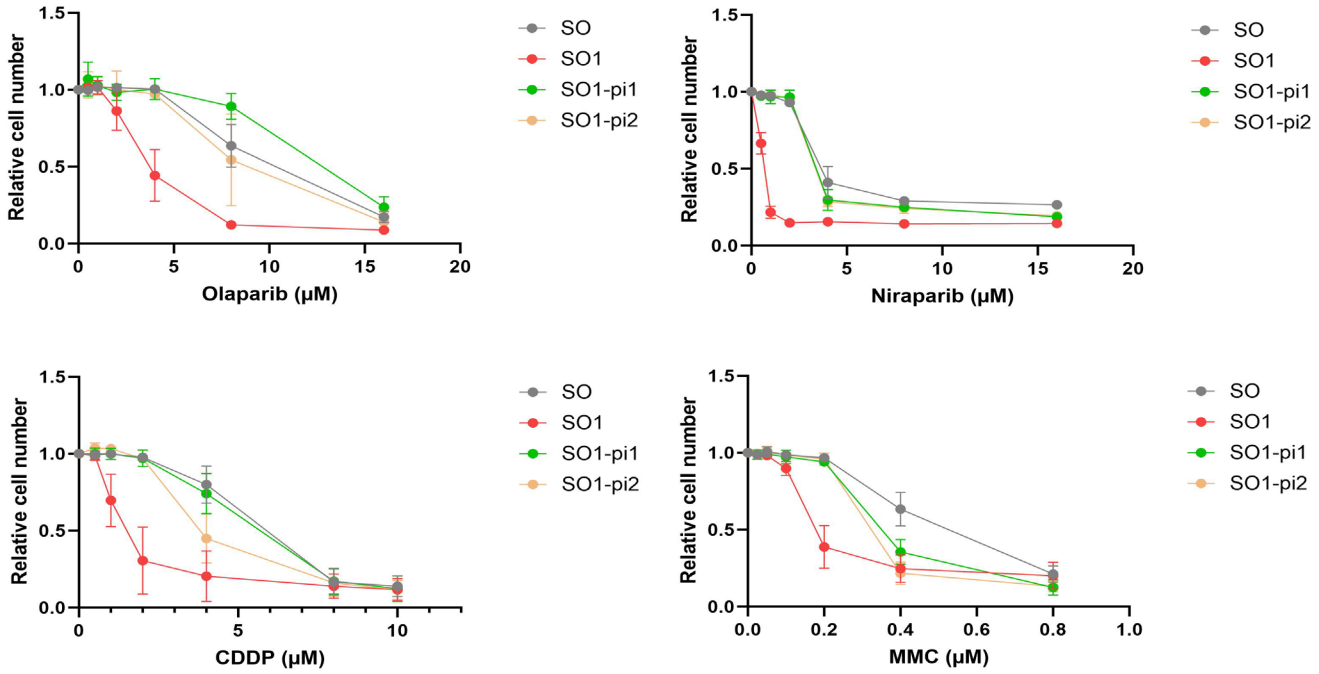

Sensitivity of olaparib resistant SO1 cells to different DNA damaging agents

Publications

TARGETED THERAPIES, ONCOGENES, GENE REGULATION, METABOLISM, CANCER PROGRESSION

1. Xing D, and Orsulic S (2005). A genetically defined mouse ovarian carcinoma model for the molecular characterization of pathway-targeted therapy and tumor resistance. Proc Natl Acad Sci U S A 102, 6936.
2. He L, Guo L, Vathipadiekal V, Sergent PA, Growdon WB, Engler DA, et al. (2014). Identification of LMX1B as a novel oncogene in human ovarian cancer. Oncogene 33, 4226.
3. Watanabe T, Marotta M, Suzuki R, Diede SJ, Tapscott SJ, Niida A, et al. (2017). Impediment of Replication Forks by Long Non-coding RNA Provokes Chromosomal Rearrangements by Error-Prone Restart. Cell Rep 21, 2223.
4. Aspuria PJ, Lunt SY, Varemo L, Vergnes L, Gozo M, Beach JA, et al. (2014). Succinate dehydrogenase inhibition leads to epithelial-mesenchymal transition and reprogrammed carbon metabolism. Cancer Metab 2, 21.
5. Miao J, Wang Z, Provencher H, Muir B, Dahiya S, Carney E, et al. (2007). HOXB13 promotes ovarian cancer progression. Proc Natl Acad Sci U S A 104, 17093.
6. Taylan E, Zayou F, Murali R, Karlan BY, Pandol SJ, Edderkaoui M, et al. (2020). Dual targeting of GSK3B and HDACs reduces tumor growth and improves survival in an ovarian cancer mouse model. Gynecol Oncol *159* , 277.
7. Chaudhuri D, Orsulic S, and Ashok BT (2007). Antiproliferative activity of sulforaphane in Akt-overexpressing ovarian cancer cells. Mol Cancer Ther *6* , 334.
8. Daikoku T, Wang D, Tranguch S, Morrow JD, Orsulic S, DuBois RN, et al. (2005). Cyclooxygenase-1 is a potential target for prevention and treatment of ovarian epithelial cancer. Cancer Res *65* , 3735.
9. Daikoku T, Tranguch S, Chakrabarty A, Wang D, Khabele D, Orsulic S, et al. (2007). Extracellular signal-regulated kinase is a target of cyclooxygenase-1-peroxisome proliferator-activated receptor-delta signaling in epithelial ovarian cancer. Cancer Res *67* , 5285.

BRCA1, PARP INHIBITORS

10. Xing D, and Orsulic S (2006). A mouse model for the molecular characterization of Brca1-associated ovarian carcinoma. Cancer Res 66, 8949.
11. Ibrahim N, He L, Leong CO, Xing D, Karlan BY, Swisher EM, et al. (2010). BRCA1-associated epigenetic regulation of p73 mediates an effector pathway for chemosensitivity in ovarian carcinoma. Cancer Res 70, 7155.
12. Goldberg MS, Xing D, Ren Y, Orsulic S, Bhatia SN, and Sharp PA (2011). Nanoparticle-mediated delivery of siRNA targeting Parp1 extends survival of mice bearing tumors derived from Brca1-deficient ovarian cancer cells. Proc Natl Acad Sci U S A 108, 745.
13. Yazinski SA, Comaills V, Buisson R, Genois MM, Nguyen HD, Ho CK, et al. (2017). ATR inhibition disrupts rewired homologous recombination and fork protection pathways in PARP inhibitor-resistant BRCA-deficient cancer cells. Genes Dev 31, 318.
14. Huang J, Wang L, Cong Z, Amoozgar Z, Kiner E, Xing D, et al. (2015). The PARP1 inhibitor BMN 673 exhibits immunoregulatory effects in a Brca1(-/-) murine model of ovarian cancer. Biochem Biophys Res Commun 463, 551.

IMMUNE THERAPIES, VACCINES

15. Righi E, Kashiwagi S, Yuan J, Santosuosso M, Leblanc P, Ingraham R, et al. (2011). CXCL12/CXCR4 blockade induces multimodal antitumor effects that prolong survival in an immunocompetent mouse model of ovarian cancer. Cancer Res 71, 5522.
16. Mantia-Smaldone G, Ronner L, Blair A, Gamerman V, Morse C, Orsulic S, et al. (2014). The immunomodulatory effects of pegylated liposomal doxorubicin are amplified in BRCA1--deficient ovarian tumors and can be exploited to improve treatment response in a mouse model. Gynecol Oncol 133, 584.
17. Yuan J, Kashiwagi S, Reeves P, Nezivar J, Yang Y, Arrifin NH, et al. (2014). A novel mycobacterial Hsp70-containing fusion protein targeting mesothelin augments antitumor immunity and prolongs survival in murine models of ovarian cancer and mesothelioma. J Hematol Oncol 7, 15.
18. Wang L, Amoozgar Z, Huang J, Saleh MH, Xing D, Orsulic S, et al. (2015). Decitabine Enhances Lymphocyte Migration and Function and Synergizes with CTLA-4 Blockade in a Murine Ovarian Cancer Model. Cancer Immunol Res 3, 1030.
19. Higuchi T, Flies DB, Marjon NA, Mantia-Smaldone G, Ronner L, Gimotty PA, et al. (2015). CTLA-4 Blockade Synergizes Therapeutically with PARP Inhibition in BRCA1-Deficient Ovarian Cancer. Cancer Immunol Res 3, 1257.
20. Guo J, De May H, Franco S, Noureddine A, Tang L, Brinker CJ, et al. (2022). Cancer vaccines from cryogenically silicified tumour cells functionalized with pathogen-associated molecular patterns. Nat Biomed Eng 6, 19.
21. Gasser S, Orsulic S, Brown EJ, and Raulet DH (2005). The DNA damage pathway regulates innate immune system ligands of the NKG2D receptor. Nature 436, 1186
22. Jia D, Nagaoka Y, Katsumata M, and Orsulic S (2018). Inflammation is a key contributor to ovarian cancer cell seeding. Sci Rep *8* , 12394.

C57BL/6 MODEL

23. Beach JA, Aspuria PJ, Cheon DJ, Lawrenson K, Agadjanian H, Walsh CS, et al. (2016). Sphingosine kinase 1 is required for TGF-beta mediated fibroblast to- myofibroblast differentiation in ovarian cancer. Oncotarget 7, 4167.
24. Hu Y, Recouvreux, MS, Haro M, Taylan E, Taylor-Harding B, Walts AE, Karlan BY, Orsulic S. INHBA(+) cancer-associated fibroblasts generate an immunosuppressive tumor microenvironment in ovarian cancer. npj Precision Oncology 2024; 8(1):35
25. Kasikova L et al. Mature tertiary lymphoid structures are associated with clinically relevant T cell exhaustion in ovarian cancer. Nature Communications, 2024

We grow the cells in DMEM + 10% FBS + 1% pen/strep, but they tend to grow well in almost any media and sera.
Any freezing media is good.
However, the cells don't grow well if they are too sparse (if <10% confluent, re-plate them into a smaller dish).